

# Thin Pr–Ba–Cu–O Film Antenna-Coupled THz Bolometers for Room Temperature Operation

Alexander Scheuring, Petra Thoma, Julia Day, Konstantin Il'in, Jens Hänisch, Bernhard Holzapfel, and Michael Siegel

**Abstract**—We report on the development of room temperature THz bolometers made from semiconducting  $\text{PrBa}_2\text{Cu}_3\text{O}_{7-\delta}$  (PBCO) thin films on MgO substrate. PBCO thin films show a high temperature coefficient of resistance (TCR  $\approx 1\text{--}2\%/K$ ) at low resistivity values ( $\rho \approx 2000 \mu\Omega\text{cm}$ ) in comparison to other semiconducting materials like amorphous silicon or vanadium oxide. A low resistivity enables efficient coupling to an integrated planar antenna required to couple THz radiation to micrometer sized detector elements. A detailed electrical characterization as well as radiation measurements at 0.65 THz of the 70–100 nm thick PBCO film microbridges embedded into log-spiral planar antennas have been performed. An electrical responsivity up to  $S = 33 \text{ V/W}$  and a noise equivalent power of  $\text{NEP} = 1.52 \times 10^{-10} \text{ W}/\sqrt{\text{Hz}}$  at a modulation frequency of 10 kHz limited by the measurement setup have been achieved.

**Index Terms**—Submillimeter wave measurements, THz bolometers, wideband antennas.

## I. INTRODUCTION

THE field of imaging applications at infrared (IR) frequencies was pushed remarkably during the last decades due to the outstanding progress in the development of integrated radiation sensors. Existing semiconductor technologies allow reliable fabrication of micro-bolometer arrays for the development of IR multi-pixel systems. Excellent results at mid-IR wavelengths have been achieved for micro-bolometers made from  $\text{VO}_x$  [1], a-Si [2], a-YBCO [3] or SiGe [4], [5] because of their high temperature coefficient of resistance  $\text{TCR} = R^{-1}dR/dT \approx 2\text{--}5\%/K$ . Such devices consist of free-standing membranes with a lateral size up to  $100 \times 100 \mu\text{m}^2$ . Radiation is directly absorbed in the membrane which is weakly coupled to the heat sink. The weak thermal coupling combined with the high TCR of the above-mentioned detector materials results in a responsivity up to several  $\text{kV/W}$  [1]–[5]. Disadvantages of membrane structures are the complex fabrication process and a long (ms range) detector response time. At the transition from the infrared to the THz frequency range, an additional problem becomes obvious: The wavelengths become comparable or even larger than the

geometrical dimensions of absorber elements, which results in a low radiation absorption.

A proven concept to realize a high radiation absorption over a wide frequency range is the use of planar antennas. There is a variety of antenna designs like dipoles, double-slot or spiral antennas specified for particular applications [6]. Most of these antennas exhibit an impedance in the order of  $Z_{\text{ant}} \approx 10\text{--}100 \Omega$ , depending on the particular geometry and on the microwave properties of the substrate. However, the impedance of semiconducting bolometers is extremely high ( $Z_{\text{det}} \approx \text{k}\Omega\text{--}\text{M}\Omega$ ) which results in high reflection losses at the interface between antenna and detector due to the significant impedance mismatch. To overcome this problem, thin metal films have been deployed for the realization of antenna-coupled bolometric detectors. Due to the low resistivity of metals it is possible to achieve very good matching of the detector impedance to the impedance of the antenna.

There are two different types of antenna-coupled bolometers: Free-standing bridges and substrate-supported detectors. Comparable to the membrane structures of the IR bolometers, free-standing bridges are thermally weakly coupled to the heat sink which results in a high responsivity, but also in a slower detector response time than for substrate-supported devices. Furthermore, free-standing structures require a complex fabrication process and can be mechanically unstable. Substrate-supported detectors are easier to fabricate and very robust. Due to the stronger thermal coupling to the heat sink, such detectors have a shorter response time. However, a consequence is a lower responsivity in comparison to free-standing structures [7], [8]. Successful fabrication and operation have been demonstrated for antenna-coupled bolometers made from Nb [7], [9] and Bi [8]. Recent progress has also been reported on detectors made from YBCO showing metallic temperature dependence at room temperature [10]. Whereas metal films give the possibility for excellent impedance matching, their TCR =  $0.15\text{--}0.3\%/K$  is much smaller than that of semiconductors [8].

Therefore it is desirable to combine the advantages of both semiconductors (high TCR for high responsivity) and metals (low resistivity for antenna impedance matching) for the development of fast and sensitive THz detectors which moreover have an ultra-broad radiation bandwidth.

In this paper we focus on the investigation of substrate-supported bolometers. We have investigated thin semiconducting  $\text{PrBa}_2\text{Cu}_3\text{O}_{7-\delta}$  (PBCO) films as a possible candidate for THz detection at room temperature. PBCO is usually used as a buffer layer for lattice matching between superconducting  $\text{YBa}_2\text{Cu}_3\text{O}_{7-\delta}$  layer and non-perovskite substrates [11]. Due

to its semiconducting nature, PBCO exhibits a high temperature coefficient of resistance which was found to be 1–2%/K for our films. This value is about one order of magnitude higher in comparison to that of metals. Furthermore, the resistivity of PBCO ( $\rho = 1000 - 2500 \mu\Omega\text{cm}$ ) is much lower than that of other semiconductors resulting in a significant reduction of the impedance in comparison to a-Si or  $\text{VO}_x$  devices of the same dimensions. Hence, it is possible to integrate PBCO detectors into planar antennas without the disadvantage of high reflection losses.

## II. ANTENNA DESIGN AND RESULTS OF SIMULATION

Planar antennas exist in different geometries and have been used successfully for a multitude of terahertz detectors like superconducting hot-electron bolometer mixers [12], photoconductive switches [13], Schottky diode detectors [14]. Since in many cases a wide radiation bandwidth is required, ultra-wide-band concepts like angular antennas or self-similar antennas are commonly used [6]. In our case a logarithmic spiral antenna was deployed. The antenna consists of two spiral-shaped arms which are connected by the detector bridge in the center of the structure. The advantage of this antenna type is a nearly frequency independent real impedance whereas the imaginary part is approximately zero. The antenna was designed to cover a frequency range from 0.2 to 2.5 THz. The layout of the antenna is shown in Fig. 1. The electromagnetic properties of the planar antenna on a magnesium oxide (MgO) substrate (thickness  $t_{\text{sub}} = 330 \mu\text{m}$ , permittivity  $\epsilon_r = 10.0$ ) were analyzed by numerical simulations [15]. The spiral antenna has a circular polarization, the mean value of the antenna impedance is approximately  $Z_A \approx 60 \Omega$ . For an estimation of the coupling efficiency between antenna and detector we have assumed an rf-impedance of the detector element which is equivalent to the dc-resistance, in our case ranging from 80 to 220  $\Omega$  (see Section III). The dependence of the simulated reflection parameter  $|S_{11}|$  on frequency is shown in Fig. 2 for both boundary values of the detector impedance. According to the nearly frequency independent input impedance of the spiral antenna, the reflection parameter exhibits a flat characteristic for frequencies above the lower cut-off value ( $f > 0.2$  THz). From these simulations the coupling efficiency between planar antenna and detector can be calculated as

$$\eta_{\text{mis}} = 1 - |S_{11}|^2 \quad (1)$$

in our case ranging from  $\eta_{\text{mis}} = 68\%$  to  $\eta_{\text{mis}} = 98\%$ . For comparison, the coupling efficiency between the antenna and a  $\text{VO}_x$  bolometer with a resistance of 27 k $\Omega$  (see [1]) results in a coupling efficiency as low as 0.9%.

The radiation properties of the planar antenna combined with a 12 mm-diameter extended hemispherical silicon lens ( $\epsilon_r = 11.7$ ), with an extension length of 1.7 mm, were analyzed by calculation of the diffraction integral according to [16]. The use of a lens improves radiation coupling by focusing the incident beam to the planar feed antenna. Furthermore, the propagation of leaky substrate modes is suppressed. The calculated directivity is  $D = 31$  dBi and the radiation coupling efficiency between the lens antenna and a Gaussian beam at 0.65 THz, with

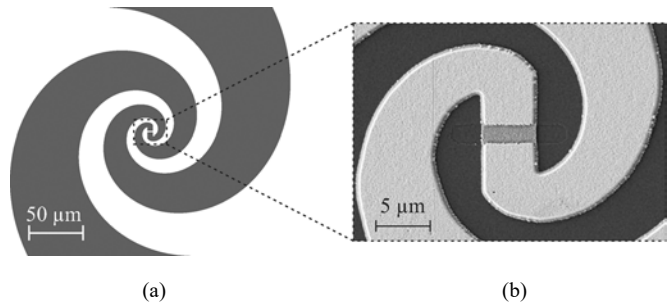


Fig. 1. (a) Layout of the logarithmic spiral antenna. (b) SEM image of the inner part of a fabricated device. The dark parts show the MgO substrate, the bright parts indicate the gold metallization of the antenna. At the center part the rectangular detector bridge is visible.

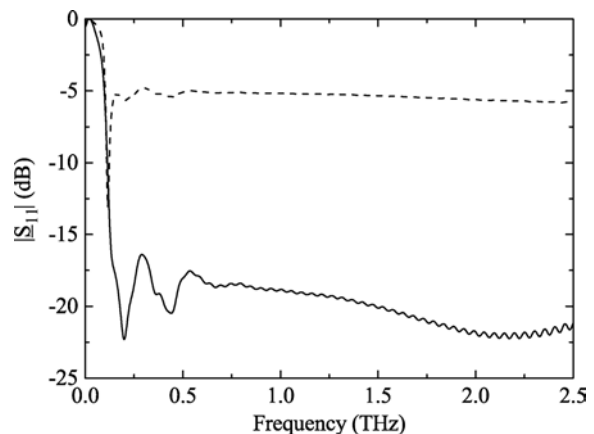


Fig. 2. Simulated reflection parameter of the planar antenna for a detector impedance of  $Z_{\text{det}} = 80 \Omega$  (solid) and  $Z_{\text{det}} = 220 \Omega$  (dashed). The curves show a flat frequency characteristic within the design bandwidth due to the nearly constant antenna input impedance.

a beam waist of  $w_0 = 0.7$  mm (see Section IV-B), was determined to  $\eta_{\text{rad}} = 42\%$ .

## III. DEVICE TECHNOLOGY AND FABRICATION

The PBCO thin films were made by pulsed laser deposition (PLD) technique. The PBCO films were grown on both-side polished magnesium oxide substrates (MgO shows low dielectric losses). After mounting of the substrate on the heater, the chamber was pumped down to a base pressure of  $5 \cdot 10^{-7}$  mbar. The PBCO films with a thickness of 70–100 nm were deposited at a heater temperature of 830 °C and an oxygen pressure of  $p_{\text{O}_2} = 0.9$  mbar with a deposition rate of 0.7 nm/s. After annealing in 900 mbar oxygen, the films were cooled down to room-temperature. Then, a Au layer with a thickness of 140 nm was grown *in situ* also with pulsed laser deposition at a pressure of  $5 \cdot 10^{-5}$  mbar. Details concerning the PLD technique used in this work are described elsewhere and can be found in [11], [17].

The films were patterned using electron-beam lithography. The detector widths  $w$  and lengths  $l$  were in the range of 2–6  $\mu\text{m}$ . To reveal the detecting element, the Au was etched using a  $\text{I}_2\text{KI}$ -wetetchant. The antenna and coplanar readout line was etched by Ar ion milling. The detector bridges showed a dc-resistance between 80 and 220  $\Omega$ , depending on film thickness and lateral dimensions.

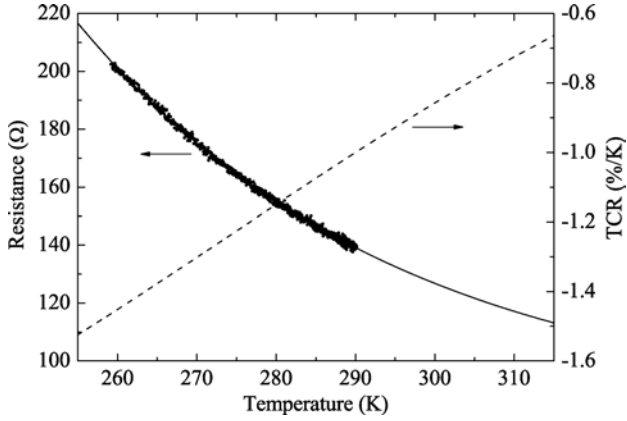


Fig. 3. Temperature dependence of detector resistance (symbols). The solid line is an exponential fit. The dashed curve is the corresponding temperature coefficient of resistance.

## IV. EXPERIMENTAL RESULTS

### A. Electrical Characterization

An important characteristic of the detector performance is the electrical responsivity  $S_{el}$ . The responsivity relates the detector output signal  $\Delta U_{sig}$  to the change of the RF-power  $\Delta P_{rf}$  that is absorbed in the detector bridge. The responsivity depends on the electrical parameters of a detector [18]:

$$S_{el} = \frac{\Delta U_{sig}}{\Delta P_{rf}} = \frac{TCR \cdot I_b \cdot R}{G_{eff} \cdot \sqrt{1 + (\omega\tau)^2}} \approx \frac{TCR \cdot I_b \cdot R}{G_{eff}} \Big|_{\omega\tau \ll 1} \quad (2)$$

Hereby,  $I_b$  is the bias current,  $R$  is the detector resistance at the operating point,  $\omega$  is the modulation frequency and  $\tau$  is the detector time constant. The effective thermal conductance of the PBCO bolometer to the MgO substrate is calculated to be  $G_{eff} = G - TCR \cdot I_b^2 \cdot R$ , where  $G$  is the thermal conductance when no current is applied. The contribution of diffusion cooling, i.e. cooling due to heat flow along the film to the antenna leads, can be neglected because the thermal conductivity of PBCO [19] is more than one order of magnitude smaller compared to Nb room-temperature devices, where thermal diffusion has to be taken into account. Furthermore, the cross-section of the diffusion channel (width  $\times$  thickness of the detector bridge) is more than one order of magnitude smaller than the cross-section of the phonon cooling channel (width  $\times$  length of the detector bridge).

The temperature dependence of resistance of the fabricated devices was investigated by a four probe measurement within the temperature range of  $T = 260\text{--}295$  K. Due to the semiconducting properties of PBCO, the resistance exhibits an exponential decay with increasing temperature (see Fig. 3). In contrast to metal bolometers, the TCR value of PBCO depends strongly on temperature. Because of the exponential decay of the resistance curve, the temperature coefficient is negative and the absolute values are decreasing with increasing temperature (see Fig. 3). For the fabricated detectors, the temperature coefficient of resistance at room temperature was in the range  $|TCR| \approx 0.8\text{--}1.3\%/K$ , which is significantly higher in comparison to metals [8].

The thermal conductance can be determined from the heat balance equation describing the behavior of a bolometer [20]:

$$C \frac{dT}{dt} = P_{el}(t) + P_{rf}(t) - G(T - T_0) \quad (3)$$

where  $T$  is the operation temperature of the bolometer,  $T_0$  is the temperature of the heat sink (here:  $T_0 = 295$  K) and  $C$  is the thermal capacitance of the bolometer. The power level depends on the absorbed radiation power  $P_{rf}$  and on the electrical power  $P_{el}$  of the applied dc bias current. For the static case ( $dT/dt = 0$ ), (3) can be rewritten in the following way:

$$G = \frac{P_{el} + P_{rf}}{T - T_0} = \frac{R(T) \cdot I_b^2 + P_{rf}}{T - T_0} \quad (4)$$

For the experimental characterization of the thermal conductance, a 1-GHz continuous wave signal was applied to the detector from a synthesizer. Bias current and rf-signal were combined with a bias-tee and coupled to the detector block by a coaxial cable. For the determination of the thermal conductance of the bolometer according to (4) the dc resistance of the bolometer was determined by a 2-wire resistance measurement and the bolometer temperature was determined from the previously acquired  $R - T$ -characteristic. The dependence of the thermal conductance  $G$  on the detector area  $A$  is shown in Fig. 4. The values are in the range from 150 to 400  $\mu W/K$  and somewhat higher than values reported for Nb and YBCO bolometers (see Table I). A linear fit was applied to these data, which results in a relation between thermal conductance and detector area in the way  $G = (14.1 \pm 0.9) \mu W/(\mu m^2 K) \times A$ . According to this dependence, we have determined an average value of the thermal boundary resistance of

$$R_{bd} = \frac{A}{G} = 7.1 \times 10^{-4} \frac{cm^2 K}{W} \quad (5)$$

A comparison with different detector types is shown in Table I. The boundary resistance value of the PBCO bolometer is comparable to the value reported for the Nb technology. In order to achieve a further reduction of the thermal conductance  $G$  for an improved detector responsivity, it is planned to increase the thermal boundary resistance by introducing an insulating buffer layer between the substrate and the PBCO film in the deposition process. Additionally, the detector area will be reduced, comparable to the suggestion in [10]. In this context, it should be mentioned that an increase of the detector response time has to be taken into account as a consequence of the stronger thermal decoupling of the PBCO bolometer from the substrate.

For the characterization of the electrical responsivity, the measurement setup was extended by an additional rf-switch that was included between synthesizer and bias-tee to modulate the RF-signal. This enables the use of a lock-in amplifier for recording the detector signals. We have analyzed the dependence of responsivity on bias current for an RF-power setting of  $-10$  dBm. Absorption losses of cables, bias-tee and RF-switch were taken into account as well as the operating point dependent reflection losses due to impedance mismatch between the detector and the  $50 \Omega$  readout electronic circuitry. The measured electrical responsivity of a  $2 \times 5 \mu m^2$  detector is shown in Fig. 5 by symbols. The responsivity shows a

TABLE I  
OVERVIEW OF UNCOOLED ANTENNA-COUPLED SUBSTRATE-SUPPORTED BOLOMETERS

Detector type	TCR (%/K)	$G$ ( $\mu\text{W/K}$ )	$R_{bd}$ ( $\text{cm}^2 \text{K/W}$ )	$S$ (V/W)	NEP ( $\text{W/Hz}^{1/2}$ )
YBCO on $\text{CeO}_2/\text{Sapphire}$ [10]	0.26	53	$3.8 \times 10^{-4}$	15	$4.5 \times 10^{-10}$
Nb on $\text{SiO}_2$ [7]	0.15	125	$8 \times 10^{-4}$	1.9	-
Bi on glass [8]	0.3	70	$2 \times 10^{-3}$	10	$2 \times 10^{-10}$
Present work (PBCO on MgO)	1.3	150	$7.1 \times 10^{-4}$	33	$1.5 \times 10^{-10}$

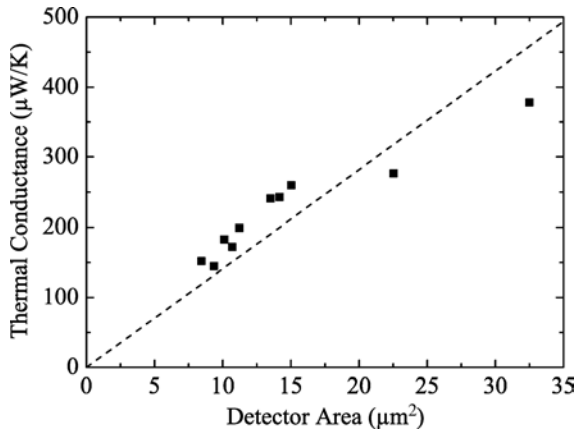


Fig. 4. Dependence of thermal conductance  $G$  (symbols) on detector area  $A$ . The dashed line is a linear fit (see text for details).

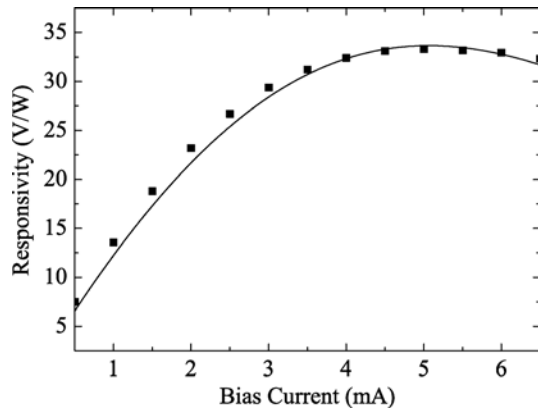


Fig. 5. Dependence of electrical responsivity of the PBCO detector on bias current (symbols). The solid line is the calculated responsivity by (2).

nonlinear dependence on the bias current with a maximum at the bias current  $I_{b_0} = 5$  mA. The nonlinear dependence can be explained by the change in temperature, generated by Joule heating of the bias current, that in turn results in a change of resistance, temperature coefficient of resistance, and of the effective thermal conductance between PBCO bolometer and the heat sink. In addition to the measurements, the responsivity values were calculated from the electrical parameters following (2) (solid line in Fig. 5). The comparison between measurement and calculation shows an excellent agreement. We have found a maximum responsivity of  $S_{\text{max}} = 33$  V/W, exceeding that

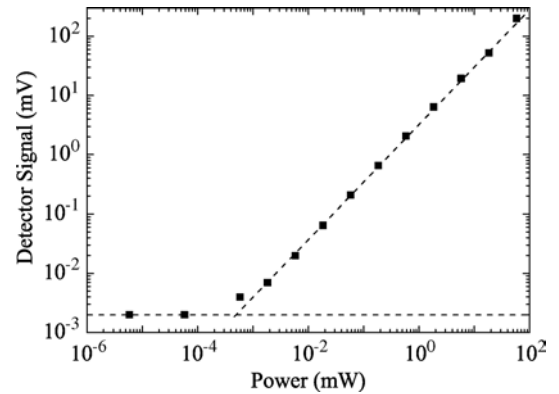


Fig. 6. Measured detector signal as a function of the microwave power. The dashed horizontal line indicates the noise level, the dashed tilted line is to guide the eye. The dynamic range is about 45 dB.

of other substrate-supported antenna-coupled bolometers made from Nb, Bi or YBCO. A comparison of the different detector technologies is shown in Table I.

For the analysis of the dynamic range, the detector element was biased with a current corresponding to its maximum responsivity while the power of the synthesizer was tuned over a large range from 1 nW to 100 mW. The detector response is linear over a wide range of more than 45 dB (Fig. 6). However, the upper power limit was determined by the saturation limit of the RF-switch which means that the dynamic range of the detector is even higher.

We also measured the dependence of the detector response on modulation frequency of the RF-switch which was varied in the range  $f_{\text{mod}} = 1$  Hz–100 kHz. Over the entire modulation frequency range the detector response was constant indicating that the detector response time is shorter than  $\tau = 1.6$   $\mu\text{s}$  (corresponding to the maximum modulation frequency of  $f_{\text{mod}} = 100$  kHz). The exact determination of the detector response time is planned for future experiments.

In contrast to the detector signal, the noise voltage shows strong frequency dependence. As it is shown in Fig. 7, a  $1/f$ -decay can be observed up to 10 kHz. For higher frequencies an increase of the noise voltage has been observed, caused by the lock-in amplifier. The voltage peaks at 50 Hz and 100 Hz are generated by the first and second harmonic of the power line frequency. The minimum value of the noise voltage is  $U_n = 5$  nV/ $\sqrt{\text{Hz}}$  which corresponds to the noise limit of the lock-in amplifier. With the known values for the responsivity

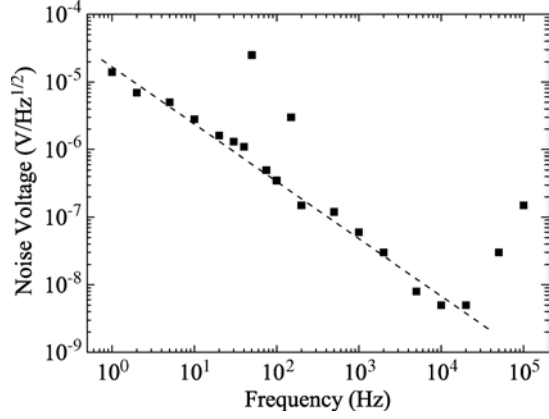


Fig. 7. Modulation frequency dependence of detector noise voltage. The noise shows a  $1/f$  decay until a frequency of 10 kHz. For higher frequencies an increase of the noise voltage was observed. The peak values at 50 Hz and 100 Hz are the first and second harmonic of the power line frequency.

and for the noise voltage the noise equivalent power (NEP) can be determined to

$$\text{NEP} = \frac{U_n}{S_{el}} \approx 1.52 \times 10^{-10} \text{ W}/\sqrt{\text{Hz}} \quad (6)$$

at a modulation frequency of 10 kHz, which was limited by the experimental setup.

### B. THz Measurements

The detector response to THz radiation was measured at 0.65 THz. For this experiment the  $3 \times 3 \text{ mm}^2$  detector chip was mounted on the extended hemispherical silicon lens. A scheme of the experimental setup is shown in Fig. 8. A frequency multiplier serves as THz source which generates a continuous wave signal that is coupled into free space by a corrugated feed horn. The beam is linearly polarized along the vertical axes and has a Gaussian shape with a beam waist of  $w_0 = 0.7 \text{ mm}$ . The diverging beam was focused by two off-axis parabolic mirrors onto the detector block which was mounted in an optical cryostat. Although no cooling is required, the use of a cryostat is helpful for optical alignment and electrical shielding. Moreover, incoming radiation is coupled into the cryostat by a HDPE window which works as filter to block infrared radiation. The radiation power level was measured with a THz power meter [21] to  $P_{\text{rad}} = 110 \mu\text{W}$  at the focal point of the second parabolic mirror. The radiation signal was modulated by a chopper wheel with a frequency of  $f_{\text{mod}} = 20 \text{ Hz}$ . The dependence of the measured THz response of the detector on bias current is shown in Fig. 9. Since a bolometer is an integrating detector which responds to the amount of absorbed power, the THz measurement shows the same characteristic as for the microwave measurements. For comparison, the signal of the 1 GHz microwave measurement at a source power level of  $-10 \text{ dBm}$  is shown. This allows us to determine the system coupling efficiency for the THz measurement setup by comparing the responsivity values. For optimum optical alignment we have measured an optical responsivity of  $S_{\text{opt}} = 1.6 \text{ V/W}$  (referred to the radiation power of the THz source). From the relation between microwave and

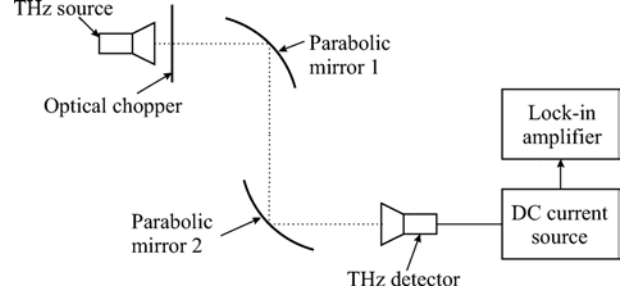


Fig. 8. Schematic of the experimental setup for radiation measurements at 0.65 THz.

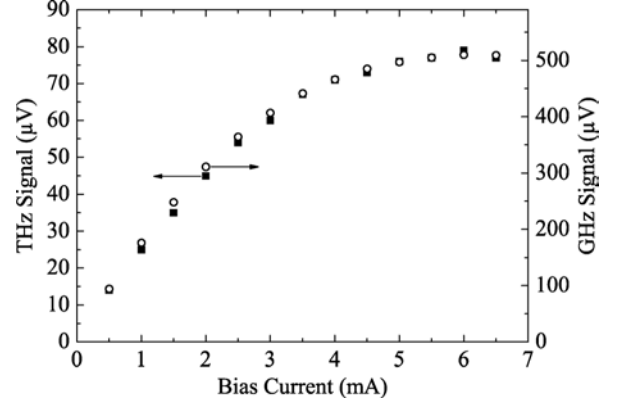


Fig. 9. Dependence of THz (solid symbols) and microwave (open symbols) response of the PBCO detector on bias current.

TABLE II  
OPTICAL PARAMETERS AT 0.65 THz

HDPE window transmission	80 %
Transmission at lens-air-interface	67 %
Gaussian beam coupling efficiency	42 %
Polarization coupling efficiency	50 %
Antenna-bolometer coupling @ $I_b=5 \text{ mA}$	71 %
<b>Total coupling efficiency</b>	<b>8 %</b>

THz measurements, the measured system coupling efficiency was determined to

$$\eta_{\text{sys}} = \frac{S_{\text{opt}}}{S_{\text{el}}} \approx 5\% \quad (7)$$

This value is in quite good agreement with the calculated system coupling efficiency of 8% according to the optical losses of the system components listed in Table II: The transmission of the HDPE window of the cryostat was determined experimentally, the other losses were calculated by numerical simulation. The difference between measured and calculated coupling efficiency can be seen in the material dependent absorption losses of lens, substrate and antenna metallization as well as imperfect alignment of the detector chip on the rear side of the lens which was not taken into account in the simulation.

## V. CONCLUSION

We have studied the performance of thin PBCO film antenna-coupled THz detectors operating at room temperature. The temperature coefficient of resistance of fabricated PBCO detectors was in the range  $\text{TCR} = 0.8\%/K - 1.3\%/K$  at  $T = 295\text{ K}$  which is much higher than that of other antenna-coupled substrate-supported bolometers made from Nb, Bi or YBCO. The resistance of the detectors was in the range  $Z_{\text{det}} = 80 - 220\ \Omega$  which enables easy antenna-coupling in contrast to highly resistive semiconductors like  $\text{VO}_x$  or a-Si. We have measured electrical responsivity values up to  $33\text{ V/W}$  and a minimum noise equivalent power  $NEP$  of  $1.52 \times 10^{-10}\text{ W/Hz}^{1/2}$  at a modulation frequency of  $10\text{ kHz}$ .

For a further improvement of the detector properties the fabrication process will be optimized with respect to a reduction of the thermal conductance. This can be realized by using an additional buffer layer between substrate and detector bridge and by a further reduction of the lateral detector dimensions.

## REFERENCES

- [1] N. Chi-Anh, H.-J. Shin, K. Kim, Y.-H. Han, and S. Moon, "Characterization of uncooled bolometer with vanadium tungsten oxide infrared active layer," *Sensors and Actuators A Phys.*, vol. 123–124, pp. 87–91, 2005.
- [2] M. Almasri, B. Xu, and J. Castracane, "Amorphous silicon two-color microbolometer for uncooled IR detection," *IEEE Sensors J.*, vol. 6, no. 2, pp. 293–300, Apr. 2006.
- [3] A. Mahmood, D. P. Butler, and Z. Celik-Butler, "Micromachined bolometers on polyimide," *Sensors and Actuators A Phys.*, vol. 132, pp. 452–459, 2006.
- [4] M. Garcia, R. Ambrosio, A. Torres, and A. Kosarev, "IR bolometers based on amorphous silicon germanium alloys," *J. Non-Cryst. Solids*, vol. 338–340, pp. 744–748, Jun. 2004.
- [5] M. M. Rana and D. P. Butler, "Radio frequency sputtered  $\text{Si}_{1-x}\text{Ge}_x$  and  $\text{Si}_{1-x}\text{Ge}_x\text{O}_y$  thin films for uncooled infrared detectors," *Thin Solid Films*, vol. 514, pp. 355–360, Aug. 2006.
- [6] C. Balanis, "Frequency independent antennas, antenna miniaturization, and fractal antennas," in *Antenna Theory Analysis and Design*. Hoboken, NJ: Wiley Interscience, 2005, pp. 611–618.
- [7] A. J. Miller, A. Luukanen, and E. N. Grossman, "Micromachined antenna-coupled uncooled microbolometers for terahertz imaging arrays," in *Proc. SPIE*, 2004, 5411, pp. 18–24.
- [8] D. P. Neikirk, W. W. Lam, and D. B. Rutledge, "Far-infrared microbolometer detectors," *Int. J. Infrared Millim. Waves*, vol. 5, pp. 245–278, Mar. 1984.
- [9] M. E. MacDonald and E. N. Grossman, "Niobium microbolometers for far-infrared detection," *IEEE Trans. Microw. Theory Techn.*, vol. 43, no. 4, pp. 893–896, Apr. 1995.
- [10] S. Cherednichenko, A. Hammar, S. Bevilacqua, V. Drakinskiy, J. Stake, and A. Kalabukhov, "A room temperature bolometer for terahertz coherent and incoherent detection," *IEEE Trans. THz Sci. Technol.*, vol. 1, no. 2, pp. 395–402, Nov. 2011.
- [11] P. Probst, A. Scheuring, M. Hofherr, S. Wunsch, K. Ilin, A. Semenov, H.-W. Hübers, V. Judin, A.-S. Müller, J. Hänisch, B. Holzzapfel, and M. Siegel, "Superconducting  $\text{YBa}_2\text{Cu}_3\text{O}_{7-\delta}$  thin film detectors for picosecond THz pulses," *J. Low. Temp. Phys.*, vol. 167, pp. 898–903, Jan. 2012.
- [12] A. D. Semenov, H. Richter, H.-W. Hübers, B. Gunther, A. Smirnov, K. S. Il'in, M. Siegel, and J. P. Karamarkovic, "Terahertz performance of integrated lens antennas with a hot-electron bolometer," *IEEE Trans. Microw. Theory Techn.*, vol. 55, no. 2, pp. 239–247, Feb. 2007.
- [13] R. Mendis, C. Sydlo, J. Sigmund, M. Feiginov, P. Meissner, and H. L. Hartnagel, "Tunable CW-THz system with a log-periodic photoconductive emitter," *Solid-State Electron.*, vol. 48, pp. 2041–2045, Oct. 2004.
- [14] A. Semenov, O. Cojocari, H.-W. Hübers, S. Fengbin, A. Klushin, and A.-S. Müller, "Application of zero-bias quasi-optical schottky-diode detectors for monitoring short-pulse and weak terahertz radiation," *IEEE Electron Device Lett.*, vol. 31, no. 7, pp. 674–676, Jul. 2010.
- [15] CST Microwave Studio 2012 [Online]. Available: <http://www.cst.com/>
- [16] D. F. Filipovic, S. S. Gearhart, and G. M. Rebeiz, "Double-slot antennas on extended hemispherical and elliptical silicon dielectric lenses," *IEEE Trans. Microw. Theory Techn.*, vol. 41, no. 10, pp. 1738–1749, Oct. 1993.
- [17] P. Probst, A. Semenov, M. Ries, A. Hoehl, P. Rieger, A. Scheuring, V. Judin, S. Wunsch, K. Il'in, N. Smale, Y.-L. Mathis, R. Müller, G. Ulm, G. Wüstefeld, H.-W. Hübers, J. Hänisch, B. Holzzapfel, M. Siegel, and A.-S. Müller, "Nonthermal response of  $\text{YBa}_2\text{Cu}_3\text{O}_{7-\delta}$  thin films to picosecond THz pulses," *Phys. Rev. B*, vol. 85, p. 174511, May 2012.
- [18] P. L. Richards, "Bolometers for infrared and millimeter waves," *J. Appl. Phys.*, vol. 76, 1994.
- [19] A. V. Inyushkin, A. N. Taldenkov, L. N. Dem'yanets, T. G. Uvarova, and A. B. Bykov, "Thermal conductivity of layered superconductors," *Phys. B Cond. Matter*, vol. 194–196, pp. 479–480, Feb. 1994.
- [20] S. Sedky, P. Fiorini, M. Caymax, A. Verbist, and C. Baert, "IR bolometers made of polycrystalline silicon germanium," *Sensors and Actuators A Phys.*, vol. 66, pp. 193–199, Apr. 1998.
- [21] QMC Instruments Ltd. [Online]. Available: <http://www.tera-hertz.co.uk/>

**Alexander Scheuring** received the Diploma Degree in electrical engineering and information technologies from the University of Karlsruhe, Germany, in 2007.

In April 2007, he joined the Institute of Micro- and Nanoelectronic systems, University of Karlsruhe (later Karlsruhe Institute of Technology). He works on the design and development of quasi-optical receiver concepts for superconducting THz radiation detectors. From February 2008 to July 2008, he was with the LGEP-Supelec in Paris, France, where he was involved in the development of ultra-wideband high-impedance antennas for semiconducting room-temperature THz bolometers.

**Petra Thoma** received the Diploma degree in electrical engineering and information technologies from the Karlsruhe Institute of Technology, Germany, in 2009.

In November 2009, she joined the Institute of Micro- and Nanoelectronic systems, Karlsruhe Institute of Technology. Her main research area is the development of high-temperature YBCO superconducting detectors for ultra-fast pulse measurements in the THz frequency range. These detectors are used for the characterization of picosecond THz pulses emitted at electron storage rings.

**Julia Day** received the Diploma degree in electrical engineering and information technologies from the Karlsruhe Institute of Technology, Germany, in 2012.

From June 2011 to October 2011, she was working at the Institute of Photonic Technology in Jena, Germany, where she was involved in the development of a process for atomic layer deposition of superconducting NbN. Her diploma thesis was about the optimization of PBCO thin film technology for integrated THz detectors.

**Konstantin Il'in** was born in Moscow, Russia, on March 24, 1968. He received the Ph.D. degree in solid-state physics from Moscow State Pedagogical University (MSPU), Moscow, Russia, in 1998.

From 1997 to 1998, he was a Visiting Scientist with the Electrical and Computer Engineering Department, University of Massachusetts at Amherst, and with the Electrical Engineering Department, University of Rochester, Rochester, NY. From January 1998 to June 1999, he was an Assistant Professor with the Physics Department, MSPU. From 1999 to 2003, he was a Scientific Researcher with the Institute of Thin Films and Interfaces, Research Center Juelich, Juelich, Germany. In June 2003, he joined the Institute of Micro- and Nano-electronic Systems, University of Karlsruhe, Karlsruhe, Germany, where he currently develops technology of ultrathin films of conventional superconductors for receivers of electromagnetic radiation. His research interests include fabrication and study of normal state and superconducting properties of submicrometer- and nanometer-sized structures from ultrathin films of disordered superconductors.

**Jens Hänisch** received both the Diploma Degree and the Ph.D. degree in physics from TU Dresden, Germany, in 2001 and 2005, respectively.

From 1997–1998, he was studying physics within the Erasmus program of EU at University of Sheffield, U.K.. Following the Ph.D. studies, he went for a three-year Post-Doctoral research term to the Superconductivity Technology Center at Los Alamos National Laboratory, AZ. There, he worked on the preparation and characterization of IBAD-based coated conductors and non-destructive long-length measurement tools. 2008 he joined again the group Superconducting Materials at IFW Dresden. Since then he worked mainly on pulsed laser deposition of superconducting thin films and measurements of their structural and transport properties.

**Bernhard Holzapfel** received the Ph.D. degree in physics studied physics from University of Erlangen, Erlangen, Germany, in 1995.

Since 1993 he is a permanent staff member at the Leibniz Institute for Solid State and Materials Research Dresden (IFW Dresden) working mainly on superconducting materials for energy and magnet applications as well as on Pulsed Laser Deposition of functional thin films. He spent a one year post-doctoral stay at ORNL, and since 2000 he is leading the Superconducting Materials Group at the IFW Dresden. Starting from 2010 he is lecturing at the TU Bergakademie Freiberg.

**Michael Siegel** received the Diploma degree in physics and the Ph.D. degree in solid state physics from the Moscow State University, Moscow, Russia, in 1978 and 1981, respectively.

In 1981, he joined the University of Jena where he held positions as Staff Member and later as Group Leader in the Superconductive Electronic Sensor Department. His research was oriented on non-linear superconductor-semiconductor devices for electronic applications. In 1987, he initiated research at the University of Jena in thin-film high temperature superconductivity (HTS) for Josephson junction devices, mainly for SQUID. In 1991, he left to join the Institute for Thin Film and Ion Technology at Research Center Juelich. There he worked on development and application of HTS Josephson junctions, SQUID, microwave arrays and mixers, and high-speed digital circuits based on rapid-single-flux-quantum logic. In 2002, he received a Full Professor position at University of Karlsruhe, Germany, where he is now the Director of the Institute of Micro- and Nanoelectronic Systems. His research includes transport phenomena in superconducting, quantum and spin dependent tunneling devices. He has authored over 200 technical papers.

## Repository KITopen

Dies ist ein Postprint/begutachtetes Manuskript.

Empfohlene Zitierung:

Scheuring, A.; Thoma, P.; Day, J.; Il'in, K.; Hänisch, J.; Holzapfel, B.; Siegel, M.  
[Thin Pr-Ba-Cu-O film antenna-coupled THz bolometers for room temperature operation.](#)  
2013. IEEE transactions on terahertz science and technology, 3  
[doi: 10.554/IR/1000039996](#)

Zitierung der Originalveröffentlichung:

Scheuring, A.; Thoma, P.; Day, J.; Il'in, K.; Hänisch, J.; Holzapfel, B.; Siegel, M.  
[Thin Pr-Ba-Cu-O film antenna-coupled THz bolometers for room temperature operation.](#)  
2013. IEEE transactions on terahertz science and technology, 3 (1), 103–109.  
[doi:10.1109/TTHZ.2012.2226880](#)

Lizenzinformationen: [KITopen-Lizenz](#)